Cancer Research

Reprogramming Tumor-Associated Dendritic Cells *In Vivo* Using miRNA Mimetics Triggers Protective Immunity against Ovarian Cancer

Juan R. Cubillos-Ruiz[1], Jason R. Baird[1,2], Amelia J. Tesone[5], Melanie R. Rutkowski[5], Uciane K. Scarlett[5], Ana L. Camposeco-Jacobs[1], Jorge Anadon-Arnillas[1], Noah M. Harwood[1], Murray Korc[3,4], Steven N. Fiering[1,2], Lorenzo F. Sempere[3], and Jose R. Conejo-Garcia[5]

Abstract

Modulating the activity of miRNAs provides opportunities for novel cancer interventions. However, low bioavailability and poor cellular uptake are major challenges for delivering miRNA mimetics specifically to tumor cells. Here, we took advantage of the spontaneous enhanced endocytic activity of ovarian cancer-associated dendritic cells (DC) to selectively supplement the immunostimulatory miRNA miR-155. *In vivo* processing of nanoparticles carrying oligonucleotide duplexes mimicking the bulged structure of endogenous pre-miRNA (but not siRNA-like oligonucleotides) dramatically augmented miR-155 activity without saturating the RNA-induced silencing complex. Endogenous processing of synthetic miR-155 favored Ago2 and, to a lesser extent, Ago4 loading, resulting in genome-wide transcriptional changes that included silencing of multiple immunosuppressive mediators. Correspondingly, tumor-infiltrating DCs were transformed from immunosuppressive to highly immunostimulatory cells capable of triggering potent antitumor responses that abrogated the progression of established ovarian cancers. Our results show both the feasibility and therapeutic potential of supplementing/replenishing miRNAs *in vivo* using nonviral approaches to boost protective immunity against lethal tumors. Thus, we provide a platform, an optimized design, and a mechanistic rationale for the clinical testing of nonviral miRNA mimetics. *Cancer Res; 72(7); 1683–93. ©2012 AACR.*

Introduction

miRNAs are small endogenous noncoding RNAs implicated in the posttranscriptional control of gene expression in developmental, physiologic, and pathologic processes. Biologically active/mature miRNAs bind to partially complementary sequences [miRNA recognition element (MRE)] in hundreds of mRNAs, which diminish protein production via mRNA degradation and/or translational repression. miRNA-mediated regulation therefore constitutes a major mechanism to control global gene expression patterns (1–3).

miRNAs are quickly challenging our understanding of genetic regulation in health and disease, including cancer etiology (4) and the generation and inhibition of antitumor immune responses (5–9). Biologically active miRNAs bind to MREs on multiple mRNAs and simultaneously silence multiple target genes. This process can directly or indirectly modulate global gene expression and eventually determines transcriptional programs associated with a specific phenotype.

Because immune responses–including those against tumor antigens–depend on rapid phenotypic changes, it is not surprising that miRNAs have emerged as critical regulators of virtually all immune cell types (5, 7). miR-155 epitomizes the role of miRNAs in the immune system. miR-155 is basally expressed at low levels in B cells (7, 8), T cells (10), macrophages (11), dendritic cells (DC; ref. 7), and progenitor/stem cell populations (10). Activation signals such as antigen, toll-like receptor (TLR) stimulation and inflammatory cytokines, rapidly increase miR-155 expression in various leukocytic subsets, including bone marrow DCs (BMDC) and macrophages (7, 8, 11). Interestingly, BMDCs matured in the absence of miR-155 upregulate MHC-II and costimulatory molecules but are incapable of effectively activating T cells (7).

We previously showed that leukocytes with predominant phenotypic attributes of regulatory DCs (including the expression of CD11c and DEC205) home to perivascular locations in the ovarian cancer microenvironment, where they express multiple immunosuppressive mediators (12–14). From their position around blood vessels, these regulatory DCs inhibit the protective function of antitumor T cells infiltrating the tumor from the blood. Although specific delivery of RNA oligonucleotides to cancer cells is challenging because of low

Authors' Affiliations: Departments of [1]Microbiology and Immunology, [2]Genetics, [3]Medicine and [4]Pharmacology and Toxicology, Dartmouth Medical School, Lebanon, New Hampshire; and [5]Tumor Microenvironment and Metastasis Program, The Wistar Institute, Philadelphia, Pennsylvania

Note: Supplementary data for this article are available at Cancer Research Online (http://cancerres.aacrjournals.org/).

Current address for M. Korc, IU Simon Cancer Center, 980 W. Walnut Street, Walther Hall, R3 C528E, Indianapolis, IN 46202.

Corresponding Author: Jose R. Conejo-Garcia, Tumor Microenvironment and Metastasis Program, The Wistar Institute, 3601 Spruce Street, Philadelphia, PA 19104. Phone: 215-495-6825; Fax: 215-495-6817; E-mail: jrconejo@Wistar.org

doi: 10.1158/0008-5472.CAN-11-3160

bioavailability, poor cellular uptake, and abundant phagocytic activity of other cell types in the tumor microenvironment (15), the enhanced endocytic pathways and relative accessibility of ovarian cancer–associated myeloid leukocytes makes them ideal targets for nanocomplex-mediated delivery. Thus, we previously showed that polyethylenimine (PEI)-based nanocomplexes are selectively and avidly taken up by DCs at ovarian cancer locations, in the absence of any targeting motif (12). Using this optimized system, we now show that activity of mature miR-155 can be augmented in tumor-associated DCs by delivering novel Dicer substrate RNA duplexes that mimic the structure of endogenous precursor miR-155 hairpin (Dmi155) and that are efficiently processed *in vivo*. Replenishing miR-155 levels in tumor-associated DCs reprogrammed their immunosuppressive phenotype by modulating the expression of nearly half of the mRNAs in their transcriptome. Synthetic enhancement of miR-155 signaling in DCs boosted potent antitumor immune responses that abrogated the progression of established ovarian cancers. Our results show the feasibility of supplementing/replenishing miRNAs *in vivo* to boost antitumor immunity against aggressive, advanced, and frequently lethal tumors.

Materials and Methods

Production of PEI-based nanoparticles encapsulating DS RNA duplexes

Endotoxin-free PEI for *in vivo* experiments "*in vivo*-jetPEI" was purchased from PolyPlus Transfection. Dicer substrates (Dsi) were synthesized at Integrated DNA Technologies (IDT) using the following chimeric sequences:

Control GFP-specific Dicer substrate (GFP Dsi):
Plus: 5′ rUrGrCrArGrArUrGrArArCrUrUrCrArGrGrGrUrCrArGrCTT 3′
Minus: 5′ rArArGrCrU rGrArC rCrCrU rGrArA rGrUrU rCrArUrCrUrG rCrArUrU 3′

Control GFP-specific "bulged" Dicer substrate:
Plus: 5′ rUrGrCrArGrArUrGrArArCrUrUrCrArGrGrGrUrCrArGrCTT 3′
Minus: 5′ rArArGrCrU rGrArC rCrCrU rG rGrUrU rCrArU rCrUrGrCrArUrU 3′

siRNA-like miR-155 Dicer substrate (Dsi155):
Plus: 5′ rUrUrA rArUrG rCrUrA rArUrU rGrUrG rArUrA rGrGrGrGrUT T 3′
Minus: 5′ rArArA rCrCrC rCrUrA rUrCrA rCrArArUrUrArGrCrArUrUrA rArUrU 3′

miRNA-like bulged miR-155 Dicer substrate (Dmi155):
Plus: 5′ rUrUrA rArUrG rCrUrA rArUrU rGrUrG rArUrA rGrGrGrGrUT T 3′
Minus: 5′ rArArA rCrCrC rCrUrA rUrCrA rA rUrUrA rGrCrArUrUrA rArUrU 3′

In all cases, "r" represents a ribonucleotide and the absence of an "r" indicates a deoxynucleotide. The "plus" strand contains 2 terminal deoxynucleotides that resemble the loop of endogenous pre-miRNA and that function as cleavage signal for Dicer. The "plus" strand refers to the strand that will give rise to the mature miRNA after Dicer processing and preferential incorporation into the RNA-induced silencing complex (RISC).

To generate PEI-based nanoparticles encapsulating Dsi, 50 to 100 μg of each annealed duplex were complexed with "*in vivo*-jetPEI" at an N/P ratio of 6, following the recommendations of the manufacturer (PolyPlus Transfection). For biodistribution experiments, Dsi were fluorescently labeled in the 3′ end of the plus strand using Cy3 (IDT). Biotinylated Dsi were also chemically synthesized at IDT and include a Biotin group in the 5′ end of the "plus" strand. Thus, after intracellular processing of the Dsi, the mature form of the miRNA remains biotinylated *in vivo*.

Transfection and *in vivo* delivery of Dsi

Lipofectamine 2000 (Invitrogen) was used for *in vitro* transfection of Dsi into HEK293 cells in 96-well plates, following the recommendations of the manufacturer. For *in vivo* biodistribution, phenotypic and gene silencing experiments, mice bearing ID8-*Defb29/Vegf-A* tumors (12) for 3 to 4 weeks were intraperitoneally injected with PEI-Dsi nanoparticles (50 μg of Dsi complexed with "*in vivo*-jetPEI" at N/P 6, per mouse). In all phenotypic and functional experiments, tumor-associated DCs from mice injected with nanoparticles were sorted from ascites or peritoneal wash samples by flow cytometry on the basis of CD45, CD11c, and MHC-II positive expression.

Tumor progression experiments

Wild-type C57BL/6 mice were intraperitoneally injected with 2×10^6 parental ID8 (kindly provided by K. Robby, University of Kansas Medical Center, Kansas City, KS; ref. 16) and treatments started 15 days posttumor injection. A total of 2×10^6 aggressive ID8-*Defb29/Vegf-A* ovarian carcinoma cells were injected intraperitoneally and treatments started after 8 days. In all cases mice received 50 μg of Dsi complexed with "*in vivo*-jetPEI" at N/P 6 in glucose 5% at the indicated time points. Some experimental groups were also intraperitoneally injected with 50 μg anti-CD40 antibody (clone FGK4.5) 3 hours before administration of PEI-based nanoparticles containing Dsi.

For tumor rechallenge protection experiments, 3×10^6 $CD3^+$ T cells negatively immunopurified from the spleens of tumor-bearing mice treated with PBS (day 32 after tumor challenge) or αCD40 Ab plus Dmi155-PEI nanoparticles (day 61 after tumor challenge; treatments at days 8, 13, 18, 23, 27, and 60) were intravenously transferred into naive C57BL/6 mice previously irradiated with 300γ (5 mice per group). Twenty-four hours later mice were challenged in the flank with ID8-*Defb29/Vegf-A* ovarian carcinoma cells, as described (14). Tumor pictures were taken 25 days later. Tumor volumes were calculated by the formula $V = 0.5\,(L \times W^2)$, in which L is length and W is width.

Results

Dicer substrate RNA duplexes generate functionally active mature miR-155

miR-155 plays an important role in oncogenesis (9) but is also required for optimal antigen presentation and T-cell

activation by mature DCs (7). We found that immunosuppressive $CD45^+CD11c^+MHC\text{-}II^+$ DCs (12, 13, 17–19) sorted from advanced orthotopic ID8-*Defb29/Vegf-A* tumors, an aggressive model of ovarian cancer that recapitulates the inflammatory microenvironment of human ovarian carcinomas (13, 14, 20, 21), showed significantly reduced levels of mature miR-155 (Fig. 1A). However, *in vivo* administration of CD40 plus TLR3 agonists, which synergistically transform tumor-associated DCs from immunosuppressive to immunostimulatory (13), induced a dramatic upregulation of mature miR-155 (Fig. 1B). We therefore hypothesized that miR-155 upregulation in DCs *in vivo* at tumor locations could be the crucial event promoting their capacity to elicit therapeutic antitumor immunity.

To augment miR-155 activity, we generated novel synthetic Dicer substrate (Dsi) RNA duplexes. To become functionally active, Dsi require processing by Dicer, the same RNAse type III enzyme that processes endogenous miRNA precursors and exogenous siRNAs. In addition, Dsi exhibit markedly enhanced silencing efficiency compared with conventional 21-mer siRNA oligonucleotides (22, 23). In all cases, we designed a forward (sense) RNA strand containing the sequence of endogenous mature miR-155 followed by 2 terminal deoxynucleotides in the 3′ end. We then generated 2 structural versions for miR-155 mimetic compounds by using different passenger (antisense) strands: An internally bulged complementary strand that recapitulates the precursor miRNA hairpin (Dmi155) and a perfectly matching, siRNA-like, complementary strand (Dsi155; Fig. 1C). Control irrelevant bulged or siRNA-like Dsi designed to target GFP were also produced in parallel.

Transfection of HEK293 cells with either Dsi155 or Dmi155 led to a dramatic dose-dependent increase in the intracellular

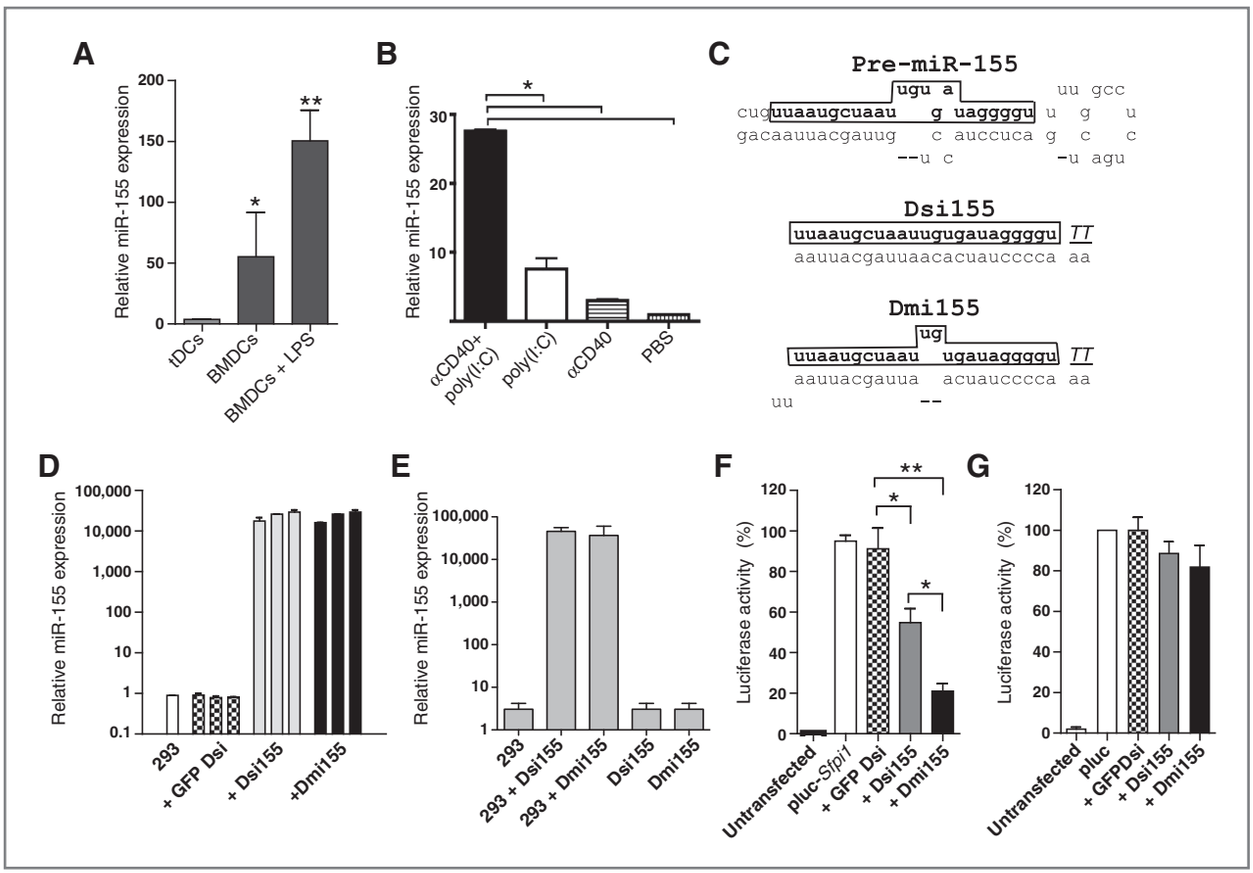

Figure 1. miR-155 expression by tumor-associated DCs and activity of RNA mimicking pre-miR-155. A, $CD45^+CD11c^+MHC\text{-}II^+$ tumor-associated DCs (tDCs) were sorted from ID8-*Defb29/Vegf-A* tumor ascites. BMDCs, generated as described (19), were stimulated with 1 μg/mL of LPS for 6 hours. Representative of 3 independent experiments. B, ID8-*Defb29/Vegf-A* tumor-bearing mice ($n = 3$) received intraperitoneal PBS, αCD40 (50 μg), poly(I:C) (100 μg), or αCD40 in combination with poly(I:C). $CD11c^+MHCII^+$ DCs were sorted from peritoneal wash after 48 hours. Representative of 2 independent experiments. C, top, endogenous pre–miR-155; middle, siRNA-like Dsi155; bottom, bulged miRNA-like Dmi155. Underlined, deoxynucleotides. Framed, mature miR-155. D, HEK293 cells in 96-well plates were transfected with 5, 10, or 25 pmol of miR-155 mimicking or control GFP-specific Dsi and 18 hours later mature miR-155 was quantified. Representative of 5 independent experiments. E, HEK293 cells in 96-well plates were transfected with 50 pmol of Dsi155 or Dmi155 and RNA was isolated 18 hours later. Fifty pmol of Dsi155 or Dmi155 were directly used as template as control. Representative of 3 independent experiments. In all cases, mature miR-155 was quantified by stem-loop qRT-PCR and data were normalized to U6 snRNA. F, a luciferase reporter vector harboring the MRE of miR-155 on *Sfpi1* was cotransfected into HEK293 cells together with different RNA duplexes. Luciferase activity in whole cell lysates was measured 24 hours later. Representative of 4 independent experiments. G, experiments were conducted as in E but using a luciferase-expressing construct without *Sfpi1* MRE. Representative of 2 independent experiments. *, $P < 0.05$; **, $P < 0.01$ (Mann–Whitney in all cases).

levels of processed miR-155, as detected by mature miRNA-specific stem-loop quantitative reverse transcriptase PCR (qRT-PCR; Fig. 1D). Confirming the selective detection of processed miRNAs by the cellular machinery, negligible signal was detected when synthetic Dsi155 or Dmi155 were directly reversed transcribed and amplified before transfection (Fig. 1E). To determine the functionality of processed miR-155 RNA generated from synthetic RNA, we cotransfected HEK293 cells with a luciferase reporter construct containing the miR-155 MRE of *Sfpi1*, an experimentally validated target gene of miR-155 (24). As expected, Dmi155 and, to a significantly lesser extent, Dsi155, rapidly silenced luciferase protein expression, whereas control (GFP specific) Dsi had no effect (Fig. 1F). Importantly, duplexes did not alter luciferase expression when the reporter constructs lacked the cognate miR-155 MRE (Fig. 1G). Together, these data showed that synthetic Dsi RNA duplexes can be used to effectively generate functionally active mature miR-155 in the cell, and suggest that a bulged structure may be important for the functionality of the miRNA generated.

Functional miR-155 delivered to tumor-associated DCs via PEI-Dsi nanocomplexes is preferentially loaded onto Ago2

We have shown that intraperitoneally injected nanocomplexes of PEI and siRNA are avidly and selectively taken up by tolerogenic DCs residing at ovarian cancer locations (12). As expected, PEI-based nanoparticles encapsulating Cy3-labeled Dmi155 were also preferentially engulfed by $CD45^+CD11c^+$ DCs in the tumor (peritoneal) microenvironment (Fig. 2A and B). Less than 1% of tumor cells incorporated the nanoparticles and only 3% of other leukocytes (primarily myeloid-derived suppressor cells and canonical macrophages) showed rhodamine fluorescence (Fig. 2B). Synthetic miR-155 was rapidly compartmentalized in the perinuclear region, typical of endosome–lysosome vesicle formation (ref. 25; Supplementary Fig. S1A). Most importantly, tumor-associated DCs endocytozing Dsi155 or Dmi155 nanocomplexes *in vivo* showed a marked increase in the intracellular levels of mature miR-155, as detected by stem-loop qRT-PCR, compared with tumor-associated DCs in mice untreated or receiving control GFP-specific Dsi (Fig. 2C). Ectopic mature miR-155 did not saturate the cellular silencing machinery because other endogenous mature miRNAs were found at comparable levels in DCs incorporating various RNA duplexes (Fig. 2D and Supplementary Fig. S1B).

To confirm the functional activity of miR-155 generated *in vivo* upon synthetic RNA processing, we analyzed the expression of 3 different experimentally validated targets of miR-155. Strikingly, the expression of *C/ebpβ* (10, 26, 27) and *Socs1* (28) was rapidly and potently silenced only in tumor-associated DCs engulfing nanoparticles of bulged Dmi155, but not perfectly matching Dsi155 or irrelevant Dsi (Fig. 2E and F). In addition, although Dsi155 induced a significant decrease in the expression of *Sfpi1* (10, 24), the silencing effect elicited by bulged Dmi155 was significantly greater (Fig. 2G). Therefore, although both Dsi155 and Dmi155 are biologically processed into mature miR-155, these data suggested that the structural features of the RNA duplex more closely mimicking the endogenous pre-miRNA hairpin are important for optimal silencing of target genes.

After Dicer processing, mature miRNAs are loaded by various Argonaute proteins (Ago1-4) into the RISC, a process that guides this multiprotein system to silence target mRNAs via cleavage, translational repression, or deadenylation (29). However, only Ago2 has slicer activity (30). Notably, we detected significantly greater amounts of mature miR-155 generated from both Dsi155 and Dmi155 by stem-loop qRT-PCR in Ago2 immunoprecipitates of peritoneal microenvironmental cells, compared with precipitation using Ago4 or, to an even lesser extent, Ago1 antibodies (Fig. 3B). Most importantly, significantly higher amounts of mature miR-155 processed from Dmi155 versus Dsi155 were found in slicer activity-endowed Ago2 pull-downs (Fig. 3B). Correspondingly, superior recovery of various known miR-155 targets was evidenced in Ago2-immunoprecipitated RNA only upon *in vivo* delivery of PEI-Dmi155, compared with administration of PEI-Dsi155 (Fig. 3C and D). Together, these results indicated that a bulged structure, similar to that of endogenous pre-miR-155, facilitates the efficient incorporation of mature miR-155 into the RISC via optimal loading onto Ago2 and, to a lesser extent, Ago4 and Ago1 proteins. There is no reliable Ago3 antibody for immunoprecipitation experiments and consequently Ago3 association studies could not be realized at this time.

Bulged Dmi155 reverts the tolerogenic activity of ovarian cancer-associated DCs and promotes their capacity to boost antitumor immunity

Because miR-155 is critical for DC-mediated antigen presentation (7) and its expression increases in response to CD40/TLR agonists, we hypothesized that delivery of miR-155 to CD40/TLR-stimulated tumor-associated DCs could further improve their antigen-presenting capacity at tumor locations. As expected, the proliferation of CFSE-labeled OT-1 T cells *in situ* in the ovarian cancer microenvironment was significantly enhanced in mice pulsed with full-length OVA when anti-CD40 plus (irrelevant) GFP Dsi-PEI nanocomplexes were administered (Fig. 4A and B). However, delivery of bulged Dmi155 induced a stronger antigen-specific T-cell proliferation at tumor locations (Fig. 4A and B), indicating that ectopic supplementation of miR-155 robustly enhances the immunostimulatory capacity of tumor-associated DCs beyond TLR activation.

Consistent with improved antigen presentation, higher proportions of antigen-experienced ($CD44^+$) $CD4^+$ and $CD8^+$ T cells were found in the tumor microenvironment of mice treated 4 times with CD40 agonists plus GFP Dsi-PEI nanocomplexes, compared with untreated mice (Fig. 4C and D and Supplementary Fig. S1C). The proportion of antigen-experienced T cells at tumor (peritoneal) locations was again further increased by treatment with PEI-complexed (bulged) Dmi155. Consistent with ineffective loading onto Ago2, the effect of perfectly matching Dsi155 was not superior to control GFP Dsi formulations (Fig. 4C and D and Supplementary Fig. S1C). Correspondingly, the number of tumor (peritoneal) T cells

secreting Granzyme B in ELISPOT analyses in response to tumor antigens was also significantly increased upon administration of bulged Dmi155, whereas treatment with siRNA-like Dsi155 did not enhance tumor antigen–specific T-cell responses more than control GFP Dsi (Fig. 4E). Likewise, mice treated with Dmi155 also showed a marked increase in the numbers of splenic T cells secreting Granzyme B upon restimulation with tumor antigens (Fig. 4F). These responses were tumor specific because they were significantly diminished when antigen-presenting cells (APC) were pulsed with irrelevant (3T3) cells in independent experiments (Supplementary Fig. S1D). Furthermore, Dmi155 treatment resulted in a significant increase in the proportions of total splenic $CD8^+$ T cells exhibiting central memory attributes ($CD44^+$ $CD62L^+$; Fig. 4G and Supplementary Fig. S1E). Finally, *in vivo* production of Th1 cytokines with antitumor potential such as TNFα, IL-12, IFNγ, and CCL5 (19, 31) was significantly enhanced at tumor locations in mice receiving Dmi155, compared with Dsi155 or control RNA (Fig. 4H). Together, these results indicated that delivery of bulged pre-miR-155 mimetic RNA, but not siRNA-like reagents, enhances the capacity of otherwise regulatory DCs at tumor locations to effectively present antigen, boost T-cell–dependent antitumor immunity, and induce the secretion of immunostimulatory cytokines

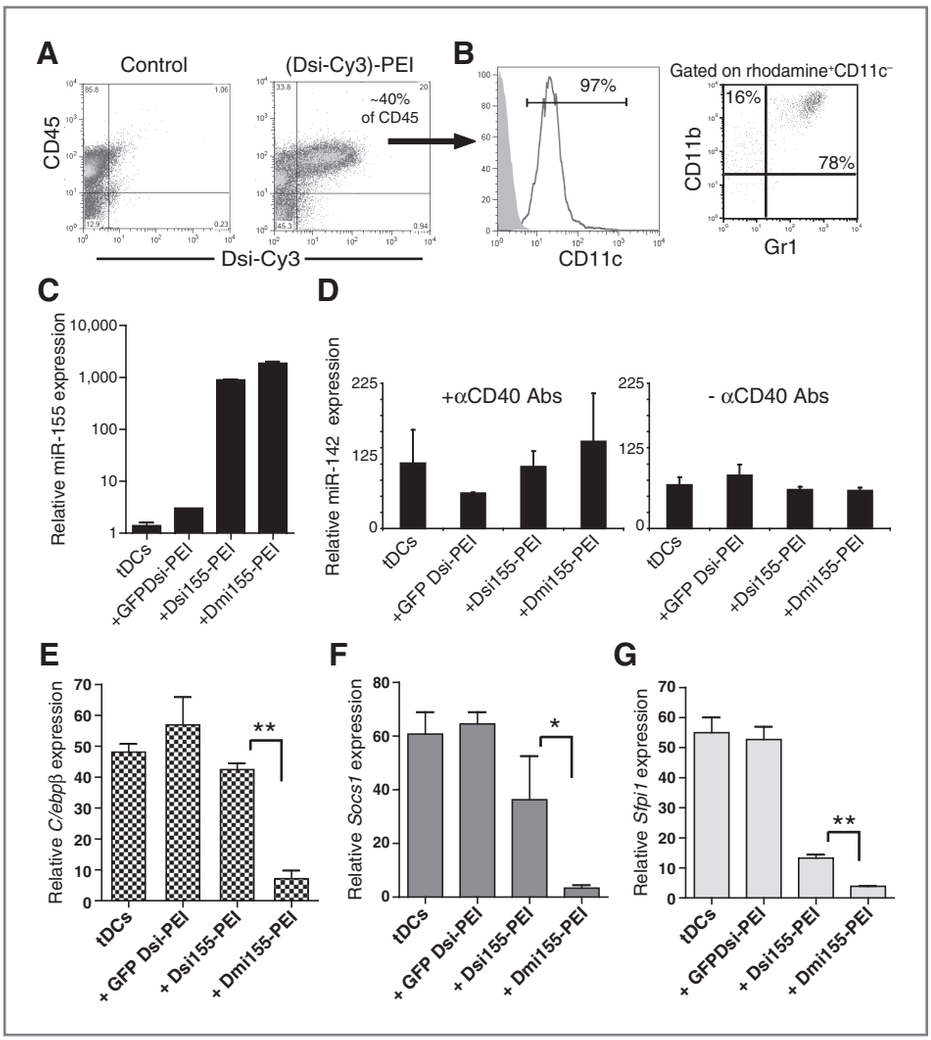

Figure 2. PEI-based nanocomplexes encapsulating functional Dmi155 are preferentially engulfed by tumor-associated DCs *in vivo*. A, Cy3-labeled Dmi155 nanocomplexes were intraperitoneally injected into mice bearing advanced ID8-*Defb29/Vegf-A* tumors. Fluorescence-activated cell sorting (FACS) analysis was done after 18 hours. Data are representative of 5 independent experiments. B, detailed analysis of leukocytes incorporating rhodamine-labeled nanocomplexes. Shaded histogram, isotype control staining. C, mice bearing advanced ID8-*Defb29/Vegf-A* ovarian tumors were left untreated or injected intraperitoneally with PEI complexed with different RNA duplexes. Eighteen hours later, $CD11c^+$MHC-II^+ tumor-associated DCs (tDCs) were sorted from peritoneal wash samples. Mature miR-155 was quantified by stem-loop qRT-PCR and the expression normalized to U6 snRNA. Data are representative of 2 independent experiments. D, mice were treated as in C or additionally injected with 50 μg of αCD40 3 hours before nanoparticle administration. miR-142-p5 expression in sorted tumor-associated DCs was quantified and normalized to U6 snRNA. E to G, expression of miR-155 mRNA targets in tumor-associated DCs engulfing PEI-Dsi nanocomplexes for 18 hours. Data were determined by qRT-PCR, normalized to glyceraldehyde-3-phosphate dehydrogenase (GAPDH) and are representative of 2 independent experiments with similar results. *, $P < 0.05$; **, $P < 0.01$ (Mann–Whitney).

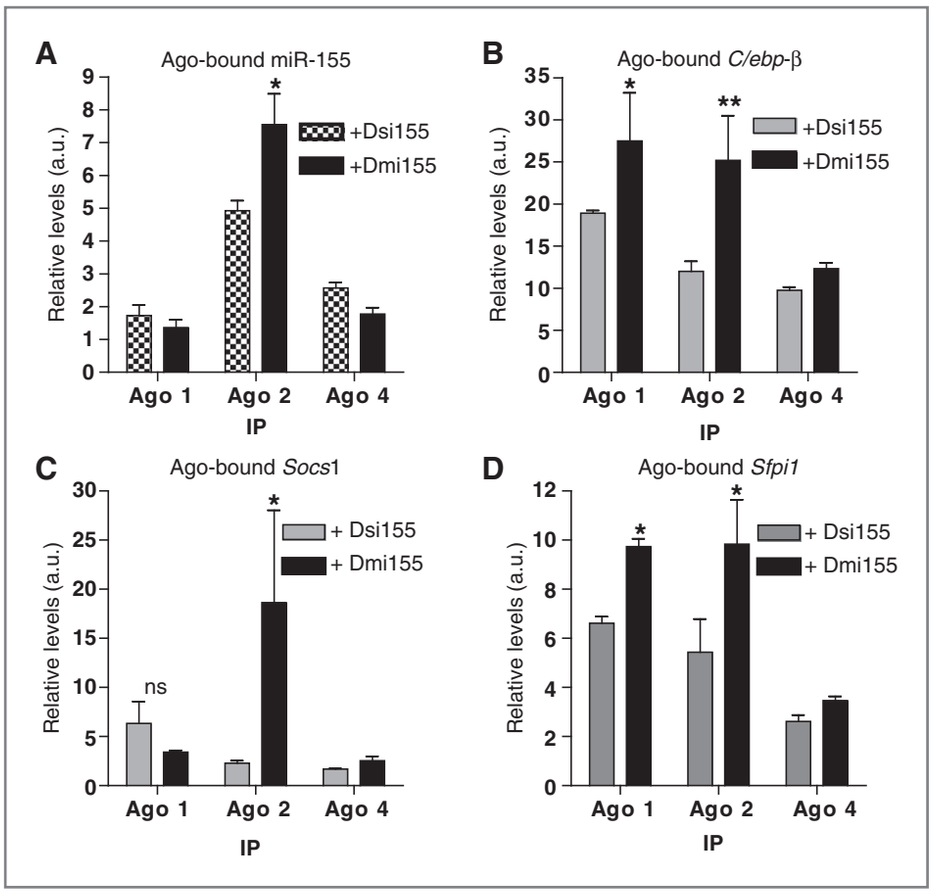

Figure 3. Loading of ectopic miR-155 onto different Ago variants. Mice bearing advanced ID8-*Defb29/Vegf-A* ovarian tumors were intraperitoneally injected with αCD40 and PEI-based nanocomplexes carrying either Dsi155, Dmi155, or control GFP-specific Dsi. Eighteen-hour postinjection, total peritoneal ascites were lysed and immunoprecipitated using monoclonal antibodies specific for Ago1, Ago2, or Ago4. Immunoprecipitated RNA was reversed transcribed and qRT-PCR was used to determine the levels of miR-155, normalized to background levels of immunoprecipitated U6 snRNA in each sample (A), and 3 known targets genes, normalized to background levels of GAPDH in each sample (B to D). *, $P < 0.05$; **, $P < 0.01$ (Mann–Whitney). IP, immunoprecipitation. a.u., arbitrary units.

beyond the sequence-independent, nonspecific activation of CD40 and TLRs (12, 13).

miR-155 delivery to tumor-associated DCs abrogates the progression of established ovarian cancer

Because tumor-associated DCs harboring increased levels of mature miR-155 exhibited functional properties of highly immunostimulatory APCs, we next determined the immunotherapeutic potential of delivering miR-155 mimetic RNA to ovarian cancer DCs, along with synergistic CD40 agonists (13). Mice growing orthotopic established ID8 ovarian tumors (16) were treated with agonistic anti-CD40 antibodies plus PEI-complexed control Dsi RNA (GFP specific), Dsi155, or Dmi155. Importantly, no obvious toxicity or secondary tumor growth in distant organs derived from the uptake of miR-155 mimetic RNA by cancer cells was observed in any case. As we previously reported (12), the intrinsic immunostimulatory activity of PEI-complexed RNA induced a significant increase of approximately 50% in the median survival of tumor-bearing mice treated with irrelevant (GFP specific) Dsi, compared with untreated mice (Fig. 5A). Consistent with the limited immunostimulatory effects on DCs, survival of mice treated with PEI-complexed Dsi155 was not superior to that elicited by the TLR5 agonist PEI alone (12), or by CD40 agonists plus the TLR5 agonist PEI, and was similar to that in mice treated with anti-CD40 antibodies plus irrelevant GFP Dsi (Fig. 5A). In contrast, treatment with bulged Dmi155 induced significantly superior effects and even abrogated disease progression in 33% of mice, which remained alive 80 days after controls succumbed to the disease (Fig. 5A). These results showed the therapeutic potential of supplementing miR-155 to tumor-infiltrating DCs *in vivo* using bulged RNA that mimics the structure of endogenous miR-155 and are consistent with the deficient silencing activity of miR-155 processed from perfectly matching oligonucleotides that merely include the sequence of mature miRNAs.

In addition, when treatments were administered to mice growing more aggressive ID8-*Defb29/Vegf-A* ovarian tumors, CD40 agonists synergized with PEI-complexed irrelevant double-stranded RNA oligonucleotides to induce a marked increase of approximately 43% in the median survival, and the effect of Dsi155 was again indistinguishable (Fig. 5B). Confirming our previous observations (13), agonistic anti-CD40 antibodies alone induce no therapeutic benefit against these tumors (Fig. 5B), unless they were combined with TLR agonists such as PEI (a TLR5 agonist; ref. 12) or double-stranded RNA. Notably, irrelevant bulged and siRNA-like Dsi targeting GFP induced identical effects (Supplementary Fig. S1F) and were, therefore, indistinctively used in subsequent experiments. Most importantly, mice receiving only 4 additional injections (days 13, 18, 23, and 27) of CD40 agonists plus PEI-complexed bulged Dmi155 exhibited a significant overall survival increase of approximately 65% compared with

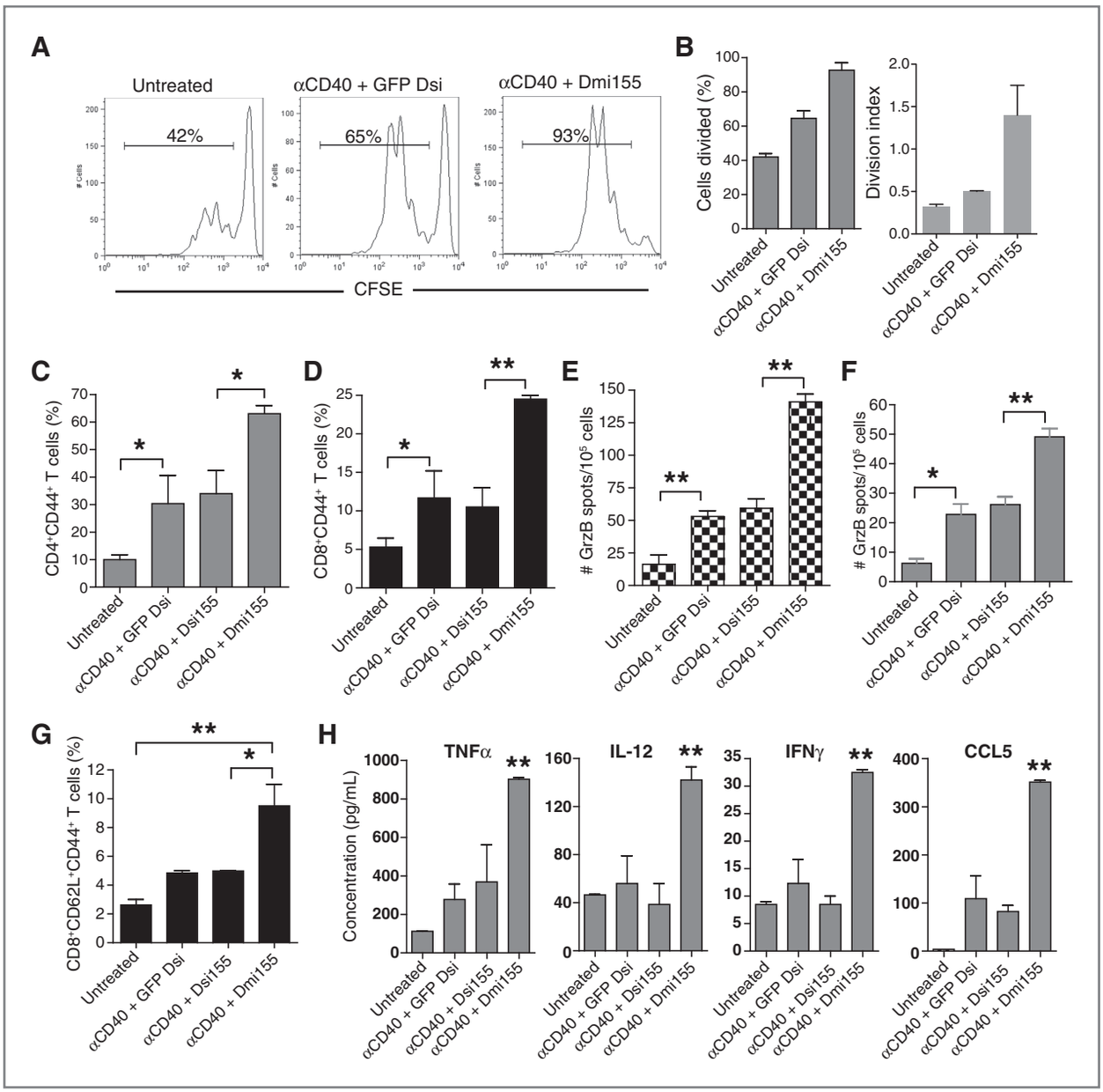

Figure 4. miR-155 delivery to tumor-associated DCs enhances antigen presentation and triggers antitumor immunity. A, mice growing ID8-*Defb29/Vegf-A* ovarian tumors for 3 weeks received 0.6 mg full-length endotoxin-free OVA (SIGMA, grade VII) intraperitoneally. Three hours later, mice were left untreated or injected with 50 μg anti-CD40 followed by 50 μg PEI-Dsi (N/P 6). Eighteen hours later, mice received 2×10^6 CFSE-labeled OVA-specific $CD3^+$ T cells negatively purified from OT-1 transgenic mice (intraperitoneally). Peritoneal wash samples (10 mL) were collected 48 hours later and T-cell proliferation was analyzed by FACS on the basis of CFSE dilution. B, left, percentage of cells divided in duplicate for each sample; right, division index of proliferating cells (FlowJo). Data are representative of 2 different mice per group. C to H, enhanced antitumor immune responses in mice treated with αCD40 plus Dmi155-PEI nanocomplexes. ID8-*Defb29/Vegf-A* tumor-bearing mice ($n = 3$ per group, 2 independent experiments) were treated at days 8, 13, 18, and 23 post tumor injection and peritoneal wash samples were analyzed at day 27. The proportion of antigen-experienced $CD4^+$ (C) and $CD8^+$ (D) T cells infiltrating tumor locations was determined by FACS (gated on $CD3^+$ cells). E and F, representative ELISPOT analysis showing increased numbers of tumor-reactive, Granzyme B–secreting T cells in the peritoneal cavity (E) or spleens (F) of mice treated with α-CD40 and Dmi155-PEI nanoparticles. GrzB, Granzyme B. G, proportion of $CD8^+$ T cells exhibiting central memory-like markers in the spleen of treated mice. H, total ascites supernatants were collected 18 hours after the administration of each indicated treatment and cytokines were measured by Bio-plex. Data are representative of 2 experiments. *, $P < 0.05$; **, $P < 0.01$ (Mann–Whitney in all cases).

untreated mice. This therapeutic effect was significantly stronger than that induced by an identical schedule of GFP Dsi-PEI or Dsi155-PEI treatments (Fig. 5B).

To confirm the antitumor effects of miR-155 mimetics in the absence of the mRNAs upregulated by CD40 activation, we finally treated aggressive tumor-bearing mice with an identical

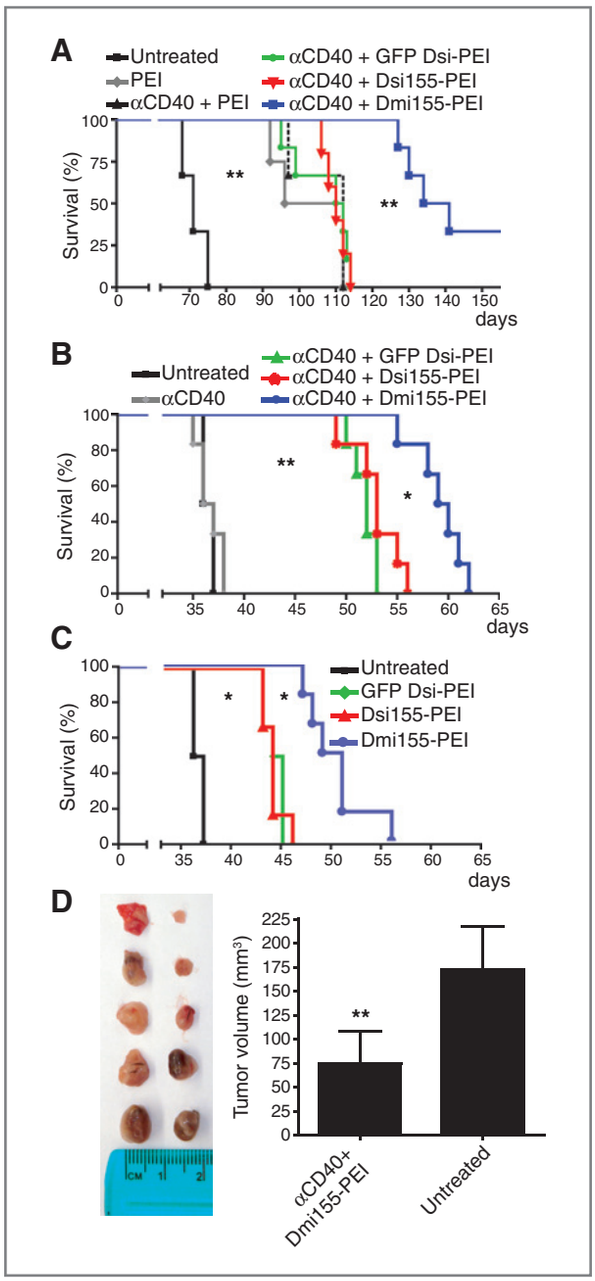

Figure 5. miR-155 delivery to tumor-associated DCs abrogates progression of established ovarian cancers. A, mice growing parental ID8 tumors (6 per group) received αCD40 antibodies and PEI-complexed Dsi at days 15, 21, 27, 28, 33, 48, and 63. Dmi155-treated mice received 2 more injections at days 114 and 129, after Dsi155-treated mice have died. ID8-*Defb29/Vegf-A* tumor-bearing mice (6 per group) were treated after 8 days with PEI–Dsi nanocomplexes in the presence (B) or absence (C) of α-CD40 agonistic antibodies. Additional treatments were given at days 13, 18, 23, and 27. D, sublethally irradiated healthy C57BL/6 mice received T cells negatively purified from the spleens of ID8-*Defb29/Vegf-A* tumor-bearing mice treated with PBS or α-CD40 agonistic antibodies plus Dmi155-PEI nanoparticles and were then challenged in the flank with the same ovarian carcinoma cells. Tumor growth in both groups was monitored 26 days later. Left, side-by-side comparison of resected tumors. Right, average tumor size in both groups.*, $P < 0.05$; **, $P < 0.01$ (log-rank or Student *t* test).

regimen of only control or miR-155 mimicking compounds. As shown in Fig. 5C, corresponding, although obviously weaker effects were observed. Notably, survival increases resulting from miR-155 supplementation were associated with T-cell–dependent protection because T cells from CD40/Dmi155-treated mice restrained tumor growth upon rechallenge, compared with T cells from untreated mice (Fig. 5D). Together, these results showed that only Dmi155 mimicking the bulged structure of endogenous pre-miR-155 is able to induce therapeutic benefits and synergize with the *in situ* activation of CD40 to extend survival in hosts bearing established aggressive ovarian carcinomas.

In vivo delivery of miR-155 mimetic RNA reprograms the transcriptome of tumor-associated DCs

To understand how mature miR-155 processed from delivered Dmi155 promotes the immunostimulatory phenotype of tumor-associated DCs in such striking manner, we next analyzed transcriptional changes in treated mice. Strikingly, deep sequencing analysis of the transcriptome of tumor-associated $CD45^+CD11c^+MHC\text{-}II^+$ DCs revealed that Dmi155, directly or indirectly, induced the silencing of thousands of transcripts, including multiple genes associated with an immunosuppressive phenotype (Supplementary File S1). Overall, 48% of total genes detected in tumor-associated DCs were downregulated 2-fold or more at the mRNA level by Dmi155 treatment. Those included known immunosuppressive targets of miR-155 such as *C/epbβ*, recently described as critical regulator of the immunosuppressive environment created by growing cancers (32); multiple mediators of Tgf-β signaling pathway, including *Tgfβ1, Smad1, Smad6*, and *Smad7*; and *Ccl22*, which recruits regulatory T cells to the tumor microenvironment (18). Unexpectedly, we also found that *Satb1*, a master genomic organizer (33), is expressed in tumor-associated DCs and silenced by miR-155.

In addition, we found downregulation of multiple transcripts not previously associated with miR-155. We focused on *Cd200*, a know mediator of DC-induced tolerance (34). Supporting that *Cd200* is indeed a *bona fide* immunosuppressive target of miR-155, luciferase activity was silenced by Dmi155, but not by irrelevant Dsi, in the presence of the 3′-untranslated region (3′-UTR) of *Cd200* (Fig. 6). The specificity of the analysis is supported by the parallel silencing of *Satb1*, recently confirmed as a target of miR-155, but not of *Pdcd4*, the expression of which is not significantly altered *in vivo* (Fig. 6).

Interestingly, *Cd200* is not a predicted target of miR-155 in any major databases. This is not surprising because 56% of published targets of miR-155 are also not contained in any major databases, including Miranda, Targetscan, DianaMT, miRDB, Mirwalk, PITA, RNA22, and PicTar.

Together, these data indicated that the transformation of plastic DCs at tumor locations into immunostimulatory cells by synthetic miR-155 is the result of complex genome-wide transcriptional changes rather than the silencing of a limited set of targets. In addition, our optimization of miRNA mimetics and delivery system provides multiple experimental hints for new targets of individual miRNAs, which should help to

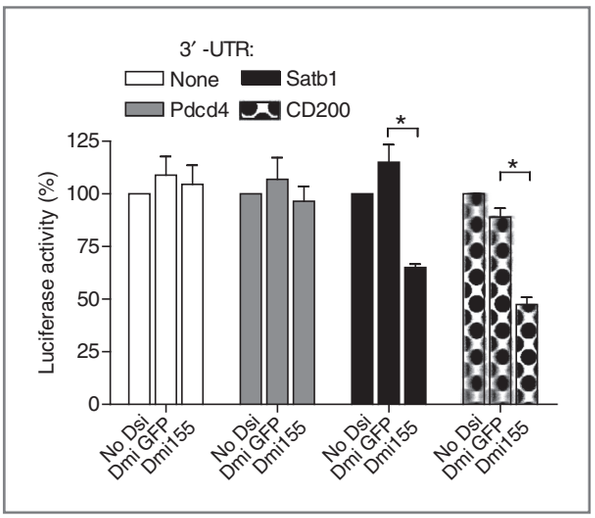

Figure 6. CD200 is a novel target of miR-155. HEK293 cells were independently cotransfected with different Dsi and reporter plasmids harboring the complete 3′-UTR region of the indicated genes (see Methods). Luciferase activity was measured 24 hours posttransfection. Data are normalized to the internal *Renilla* control in each reporter plasmid and are representative of 2 independent experiments. *, $P < 0.05$ (Mann–Whitney).

improve bioinformatical predictions by providing new clues for the design of more reliable algorithms.

Discussion

Here we show for the first time the feasibility of modulating miRNA activity selectively in ovarian cancer microenvironmental leukocytes using a nonviral approach, which promotes their capacity to elicit protective immunity.

Although expression of noncoding RNA in cancer cells can be achieved with viral vectors, the therapeutic use of viruses remains a clinical challenge. In addition, low bioavailability, poor cellular uptake, and preferential uptake by abundant phagocytic cells (15) are still major hurdles for specific delivery of genetic materials stabilized in nano- or microparticles to tumor cells. In contrast, the enhanced endocytic pathways and massive infiltration of the myeloid leukocytes that systematically accumulate in solid tumors make them ideal targets for nanocomplex-mediated delivery. Because of its relative accessibility, ovarian cancer–associated leukocytes are an ideal target for this approach.

We selected supplementing miR-155 because silencing of a nonredundant set of targets by this miRNA seems to be required for proper antigen presentation (7). However, miR-155 expression is frequently detected at high levels human cancer, both in solid tumors including breast, colorectal, lung, pancreatic, and thyroid carcinomas and in liquid tumors including lymphomas and some acute myeloid leukemias (9, 35). The association between oncogenesis and effective immunity is not surprising as robust adaptive immune responses entail rapid expansion of leukocytes. Furthermore, artificial upregulation of mir-155 leading to oncogenic conditions involves sustained overexpression in hematopoietic progenitors. In our study, the transient increase of mir-155 in lineage-committed myeloid cells such as tumor-associated DCs did not enhance ovarian cancer progression and did not result in generation of any secondary tumors. Instead, miR-155 delivery elicited robust antitumor immune responses that prolonged survival in mice bearing aggressive established ovarian cancer. Thus, miR-155 processed from endocytosed Dmi155 induced genome-wide transcriptional changes in DCs *in situ* at tumor locations, which significantly enhanced their immunostimulatory capacity. Because the expression of nearly half of the transcriptome was affected by synthetic miR-155 delivery, this significant phenotypic transformation was the result of complex coordinated transcriptional changes, rather than the silencing of a limited set of targets. Consequently, many genes known to promote tolerance were downregulated, including *C/ebpβ*, crucial immunosuppressive factor in cancer microenvironmental cells (32), and multiple mediators of the Tgfβ signaling pathway. In addition, we confirmed that other unpredicted targets of miR-155 such as *Cd200* were indeed silenced in standard luciferase assays.

Although PEI-siRNA nanocomplexes stimulate multiple TLRs on tumor-associated DCs (12), the robust enhancement in antigen presentation, production of Th1 cytokines, and expansion of tumor-reactive T cells selectively elicited by Dmi155 was significantly superior, compared with the nonspecific activation of DCs elicited by control sequences. Importantly, phenotypic transformation of DCs at tumor locations was not the result of the saturation of the RISC complex, because other mature miRNAs were clearly detected in Dmi155-treated cells. It is therefore very unlikely that the significant immunostimulatory effects, which abrogate the progression of established tumors, are the result of the sequestration of all Ago variants.

Most importantly for the clinical testing miRNA mimetics, we found that perfectly matching (siRNA-like) and bulged (miRNA-like) duplexes were both processed by tumor-associated DCs to generate mature miR-155. However, miR-155 generated from multiple batches of siRNA duplexes exhibited deficient silencing activity toward target genes *in vivo*, compared with Dmi155. Correspondingly, significantly higher amounts of mature miR-155 processed from Dmi155 versus Dsi155 were found in pull-downs of Ago2, the only Ago variant with slicer activity. miRNAs first associate with Agos as RNA duplexes that require activation, defined as conversion of the RNA duplex into a single-stranded miRNA. This activation process is the rate-limiting step in Ago loading and crucially depends on the thermodynamic instability of RNA duplexes (36). However, the cleavage activation pathway specific to Ago2 seems to be the only one insensitive to RNA thermostability in embryonic fibroblasts (36). It is possible that immune cells behave differently, so that Dmi155 and Dsi155 bind to Ago2 variants with similar affinity, but bulged duplexes with weaker thermodynamic stability are more efficiently processed and activated. Not mutually exclusive, it is also possible that chaperone proteins regulating the upload of small hairpin RNAs onto the RISC complex recognize the difference between

a bulged versus a matching structure in DCs, so that different compositions are incorporated with distinct efficiency.

In summary, our results show the feasibility of delivering synthetic miRNAs to tumor microenvironmental cells as a novel cancer intervention and provide fundamental clues for the optimization of this approach.

Disclosure of Potential Conflicts of Interest

No potential conflicts of interest were disclosed.

Authors' Contributions

Conception and design: J.R. Cubillos-Ruiz, J.R. Baird, S.N. Fiering, L.F. Sempere, and J.R. Conejo-Garcia.
Development of methodology: J.R. Cubillos-Ruiz, J.R. Baird, S.N. Fiering, L.F. Sempere, and J.R. Conejo-Garcia.
Acquisition of data (provided animals, acquired and managed patients, provided facilities, etc.): J.R. Cubillos-Ruiz, J.R. Baird, A.J. Tesone, M.R. Rutkowski, A.L. Camposeco-Jacobs, J. Anadon-Arnillas, N.M. Harwood, M. Korc, and J.R. Conejo-Garcia.
Analysis and interpretation of data (e.g., statistical analysis, biostatistics, computational analysis): J.R. Cubillos-Ruiz, J.R. Baird, A.J. Tesone, M.R. Rutkowski, J. Anadon-Arnillas, N.M. Harwood, M. Korc, S.N. Fiering, and J.R. Conejo-Garcia.
Writing, review, and/or revision of the manuscript: J.R. Cubillos-Ruiz, A.J. Tesone, M.R. Rutkowski, U.K. Scarlett, S.N. Fiering, L.F. Sempere, and J.R. Conejo-Garcia.
Administrative, technical, or material support (i.e., reporting or organizing data, constructing databases): J.R. Baird.
Generated data: U.K. Scarlett.
Study supervision: S.N. Fiering and J.R. Conejo-Garcia.

Acknowledgments

The authors thank the Bioinformatics, Genomics, Flow Cytometry, and Animal Facilities at The Wistar Institute and the Genomics and Microarray Laboratory at Dartmouth.

Grant Support

This study was supported by NCI grants CA157664, CA124515, CA124515**S**, CA132026, CA141017 and P30CA010815, and by DoD grant OC100059 (to J.R. Conejo-Garcia). J.R. Cubillos-Ruiz was supported by the 2009–2010 John H. Copenhaver, Jr. and William H. Thomas, MD 1952 Fellowship.

The costs of publication of this article were defrayed in part by the payment of page charges. This article must therefore be hereby marked *advertisement* in accordance with 18 U.S.C. Section 1734 solely to indicate this fact.

Received September 20, 2011; revised January 16, 2012; accepted January 23, 2012; published OnlineFirst February 3, 2012.

References

1. Ambros V. The functions of animal microRNAs. Nature 2004;431:350–5.
2. Bartel DP. MicroRNAs: target recognition and regulatory functions. Cell 2009;136:215–33.
3. Chi SW, Zang JB, Mele A, Darnell RB. Argonaute HITS-CLIP decodes microRNA-mRNA interaction maps. Nature 2009;460:479–86.
4. Sempere LF, Kauppinen KS. Translational implications of microRNAs in clinical diagnostics and therapeutics. 2nd edition. ed. Oxford: Academic Press.; 2009.
5. Li QJ, Chau J, Ebert PJ, Sylvester G, Min H, Liu G, et al. miR-181a is an intrinsic modulator of T cell sensitivity and selection. Cell 2007;129:147–61.
6. O'Connell RM, Rao DS, Chaudhuri AA, Baltimore D. Physiological and pathological roles for microRNAs in the immune system. Nat Rev Immunol 2010;10;111–22.
7. Rodriguez A, Vigorito E, Clare S, Warren MV, Couttet P, Soond DR, et al. Requirement of bic/microRNA-155 for normal immune function. Science 2007;316:608–11.
8. Thai TH, Calado DP, Casola S, Ansel KM, Xiao C, Xue Y, et al. Regulation of the germinal center response by microRNA-155. Science 2007;316:604–8.
9. Xiao C, Rajewsky K. MicroRNA control in the immune system: basic principles. Cell 2009;136:26–36.
10. O'Connell RM, Rao DS, Chaudhuri AA, Boldin MP, Taganov KD, Nicoll J, et al. Sustained expression of microRNA-155 in hematopoietic stem cells causes a myeloproliferative disorder. J Exp Med 2008;205:585–94.
11. O'Connell RM, Taganov KD, Boldin MP, Cheng G, Baltimore D. MicroRNA-155 is induced during the macrophage inflammatory response. Proc Natl Acad Sci U S A 2007;104:1604–9.
12. Cubillos-Ruiz JR, Engle X, Scarlett UK, Martinez D, Barber A, Elgueta R, et al. Polyethylenimine-based siRNA nanocomplexes reprogram tumor-associated dendritic cells via TLR5 to elicit therapeutic antitumor immunity. J Clin Invest 2009;119:2231–44.
13. Scarlett UK, Cubillos-Ruiz JR, Nesbeth YC, Martinez DG, Engle X, Gewirtz AT, et al. *In situ* stimulation of CD40 and toll-like receptor 3 transforms ovarian cancer-infiltrating dendritic cells from immunosuppressive to immunostimulatory cells. Cancer Res 2009;69:7329–37.
14. Conejo-Garcia JR, Benencia F, Courreges MC, Kang E, Mohamed-Hadley A, Buckanovich RJ, et al. Tumor-infiltrating dendritic cell precursors recruited by a beta-defensin contribute to vasculogenesis under the influence of Vegf-A. Nat Med 2004;10:950–8.
15. Garzon R, Marcucci G, Croce CM. Targeting microRNAs in cancer: rationale, strategies and challenges. Nat Rev Drug Discov 2010;9:775–89.
16. Roby KF, Taylor CC, Sweetwood JP, Cheng Y, Pace JL, Tawfik O, et al. Development of a syngeneic mouse model for events related to ovarian cancer. Carcinogenesis 2000;21:585–91.
17. Cubillos-Ruiz JR, Martinez D, Scarlett UK, Rutkowski MR, Nesbeth YC, Camposeco-Jacobs AL, et al. CD277 is a negative co-stimulatory molecule universally expressed by ovarian cancer microenvironmental cells. Oncotarget 2010;1:329–8.
18. Curiel TJ, Coukos G, Zou L, Alvarez X, Cheng P, Mottram P, et al. Specific recruitment of regulatory T cells in ovarian carcinoma fosters immune privilege and predicts reduced survival. Nat Med 2004;10:942–9.
19. Nesbeth Y, Scarlett U, Cubillos-Ruiz J, Martinez D, Engle X, Turk MJ, et al. CCL5-mediated endogenous antitumor immunity elicited by adoptively transferred lymphocytes and dendritic cell depletion. Cancer Res 2009;69:6331–8.
20. Conejo-Garcia JR, Buckanovich RJ, Benencia F, Courreges MC, Rubin SC, Carroll RG, et al. Vascular leukocytes contribute to tumor vascularization. Blood 2005;105:679–81.
21. Huarte E, Cubillos-Ruiz JR, Nesbeth YC, Scarlett UK, Martinez DG, Buckanovich RJ, et al. Depletion of dendritic cells delays ovarian cancer progression by boosting antitumor immunity. Cancer Res 2008;68:7684–91.
22. Kim DH, Behlke MA, Rose SD, Chang MS, Choi S, Rossi JJ. Synthetic dsRNA Dicer substrates enhance RNAi potency and efficacy. Nat Biotechnol 2005;23:222–6.
23. Rose SD, Kim DH, Amarzguioui M, Heidel JD, Collingwood MA, Davis ME, et al. Functional polarity is introduced by Dicer processing of short substrate RNAs. Nucleic Acids Res 2005;33:4140–56.
24. Martinez-Nunez RT, Louafi F, Friedmann PS, Sanchez-Elsner T. MicroRNA-155 modulates the pathogen binding ability of dendritic cells (DCs) by down-regulation of DC-specific intercellular adhesion molecule-3 grabbing non-integrin (DC-SIGN). J Biol Chem 2009;284:16334–42.
25. Chiu YL, Ali A, Chu CY, Cao H, Rana TM. Visualizing a correlation between siRNA localization, cellular uptake, and RNAi in living cells. Chem Biol 2004;11:1165–75.

26. He M, Xu Z, Ding T, Kuang DM, Zheng L. MicroRNA-155 regulates inflammatory cytokine production in tumor-associated macrophages via targeting C/EBPbeta. Cell Mol Immunol 2009;6:343–52.

27. Costinean S, Sandhu SK, Pedersen IM, Tili E, Trotta R, Perrotti D, et al. Src homology 2 domain-containing inositol-5-phosphatase and CCAAT enhancer-binding protein beta are targeted by miR-155 in B cells of Emicro-MiR-155 transgenic mice. Blood 2009;114: 1374–82.

28. Lu LF, Thai TH, Calado DP, Chaudhry A, Kubo M, Tanaka K, et al. Foxp3-dependent microRNA155 confers competitive fitness to regulatory T cells by targeting SOCS1 protein. Immunity 2009;30:80–91.

29. Winter J, Jung S, Keller S, Gregory RI, Diederichs S. Many roads to maturity: microRNA biogenesis pathways and their regulation. Nat Cell Biol 2009;11:228–34.

30. Grimm D, Wang L, Lee JS, Schurmann N, Gu S, Borner K, et al. Argonaute proteins are key determinants of RNAi efficacy, toxicity, and persistence in the adult mouse liver. J Clin Invest 2010;120: 3106–19.

31. Nesbeth YC, Martinez DG, Toraya S, Scarlett UK, Cubillos-Ruiz JR, Rutkowski MR, et al. CD4 +T cells elicit host immune responses to MHC class II- ovarian cancer through CCL5 secretion and CD40-mediated licensing of dendritic cells. J Immunol 2010;184: 5654–62.

32. Marigo I, Bosio E, Solito S, Mesa C, Fernandez A, Dolcetti L, et al. Tumor-induced tolerance and immune suppression depend on the C/EBPbeta transcription factor. Immunity 2010;32:790–802.

33. Cai S, Lee CC, Kohwi-Shigematsu T. SATB1 packages densely looped, transcriptionally active chromatin for coordinated expression of cytokine genes. Nat Genet 2006;38:1278–88.

34. Clark DA, Gorczynski RM, Blajchman MA. Transfusion-related immunomodulation due to peripheral blood dendritic cells expressing the CD200 tolerance signaling molecule and alloantigen. Transfusion 2008;48:814–21.

35. Sempere LF, Preis M, Yezefski T, Ouyang H, Suriawinata AA, Silahtaroglu A, et al. Fluorescence-based codetection with protein markers reveals distinct cellular compartments for altered MicroRNA expression in solid tumors. Clin Cancer Res 2010;16: 4246–55.

36. Gu S, Jin L, Zhang F, Huang Y, Grimm D, Rossi JJ, et al. Thermodynamic stability of small hairpin RNAs highly influences the loading process of different mammalian Argonautes. Proc Natl Acad Sci U S A 2011;108;9208–13.